T. Knöpfel and E. Boyden (Eds.)
Progress in Brain Research, Vol. 196
ISSN: 0079-6123

CHAPTER 5

Neural activity imaging with genetically encoded calcium indicators

Lin Tian*[,1], Jasper Akerboom, Eric R. Schreiter and Loren L. Looger[†]

Howard Hughes Medical Institute, Janelia Farm Research Campus, Ashburn, VA, USA

Abstract: Genetically encoded calcium indicators (GECIs), together with modern microscopy, allow repeated activity measurement, in real time and with cellular resolution, of defined cellular populations. Recent efforts in protein engineering have yielded several high-quality GECIs that facilitate new applications in neuroscience. Here, we summarize recent progress in GECI design, optimization, and characterization, and provide guidelines for selecting the appropriate GECI for a given biological application. We focus on the unique challenges associated with imaging in behaving animals.

Keywords: genetically encoded calcium indicators; protein calcium sensors; protein engineering; GCaMP3; calcium imaging; neural activity imaging.

Introduction

One of the primary challenges of neuroscience is to link complex neural phenomena to the structure and function of their composite neural circuits. Addressing this problem requires a thorough understanding of patterns of neural activity and the ability to relate this to physiological processes, behavior, and disease states. An essential step toward this goal is the simultaneous recording of neural activity in large, defined populations, ideally in intact circuitry.

Traditional electrophysiological approaches provide excellent sensitivity and temporal resolution (Scanziani and Hausser, 2009) but are limited in the number of cells that can be recorded simultaneously. More importantly, assigning this activity to specific cells is quite difficult (and impossible for more than a few cells at a time), limiting the ability to create high-resolution circuit maps. Modern fluorescence imaging techniques (Svoboda and Yasuda, 2006), combined with high-quality fluorescent indicators (both small molecules and proteins), can potentially overcome these limitations. There is

*Corresponding author.
Tel.: +571-209-4155; Fax: +571-209-4905
E-mail: lintian@ucdavis.edu
†Co-corresponding author.
E-mail: loogerl@janelia.hhmi.org

[1]Current address: Department of Biochemistry and Molecular Medicine, School of Medicine, University of California, Davis, 95817

DOI: 10.1016/B978-0-444-59426-6.00005-7

a rapidly growing toolkit of reagents that transduce changes in neural state (e.g., membrane potential or calcium ion flux, [Ca^{2+}], following action potentials (APs) or synaptic input), to fluorescence (or in some instances, luminescence, etc.) observables (for reviews, see Miyawaki, 2011; Palmer et al., 2011). Protein sensors are genetically encoded and can thus be used to label large populations of defined cell types and/or subcellular compartments (Borghuis et al., 2011; Dreosti et al., 2009; Mittmann et al., 2011; Shigetomi et al., 2010a,b), unlike small molecule dyes, whose delivery and targeting can be problematic (Hendel et al., 2008; Shigetomi et al., 2010a, b). In principle, genetically encoded sensors allow long-term measurements of activity *in vivo*, simultaneously across a neural population. Since the creation of the first generation of genetically encoded calcium indicators (GECIs), a decade ago (Miyawaki et al., 1997; Romoser et al., 1997), their performance has been iteratively optimized for applications in neurophysiology (as well as in other excitable cells such as cardiomyocytes (Tallini et al., 2006); recently, GECIs have also been used to monitor Ca^{2+} transients in nonexcitable cell types, such as astrocytes (Gourine et al., 2010; Shigetomi et al., 2010a). The culmination of these efforts has led to activity measurements of defined neuronal populations in awake, behaving animals (Chiappe et al., 2010; Dombeck et al., 2010; Lütcke et al., 2010; Muto et al., 2011; O'Connor et al., 2010; Seelig et al., 2010; Tian et al., 2009).

In neurons, APs generate small calcium transients that can occur over a wide range of frequencies. To enable quantitative measurements of neural activity, one, in principle, desires a sensor with fast rise and decay kinetics, broad dynamic range, and calcium affinity appropriate for the cells in question (Hires et al., 2008). In addition, the basal brightness of the sensor should be high enough to permit identification of positive cells and improve the signal-to-noise ratio (SNR) of baseline measurements. Improved brightness also facilitates imaging with lower excitation power, important for minimizing indicator photobleaching and illumination phototoxicity.

In this chapter, we highlight recent progress in GECI design, optimization, and testing protocol standardization. We provide guidelines for selecting the appropriate GECI for a given biological application and discuss the remaining hurdles to perfect chronic, robust neural activity imaging *in vivo*.

GECI development and neuroscience applications

The general paradigm of GECI design is to fuse a calcium-binding domain (e.g., Calmodulin, CaM, or Troponin C, TnC) to one or two fluorescent proteins (FPs). In single-FP GECIs, the fluorescence intensity of a circularly permuted or split FP is modulated by calcium binding-dependent changes in the chromophore environment (Baird et al., 1999; Nagai et al., 2001; Nakai et al., 2001). In two-FP GECIs, calcium binding allosterically modulates the relative donor–acceptor emission spectra through distance- and orientation-dependent changes in Förster resonance energy transfer (FRET) (Miyawaki et al., 1997; Heim and Griesbeck, 2004; Palmer et al., 2006). In many cases, a conformational actuator, such as the Ca^{2+}/CaM-binding peptide of myosin light chain kinase (the "M13" peptide), is included to enhance the allosteric regulation of the chromophore environment (for single-FP GECIs) or FRET (for two-FP GECIs). The molecular architecture of the major GECI classes is shown in Fig. 1.

In 1997, the first GECIs were developed by the groups of Romoser (1997) and Miyawaki (1997). FIP-CB_{SM} developed by Romoser et al., employed an avian smooth muscle myosin light chain kinase (smMLCK) M13 peptide (interestingly, a conservative point mutation, glutamine to asparagine, was inadvertently introduced), sandwiched between blue- and red-shifted versions of GFP ("BGFP" and "RGFP," respectively), and relied on endogenous CaM for modulating the FRET between the two. Cameleon developed by Miyawaki et al., included its own CaM as well as a

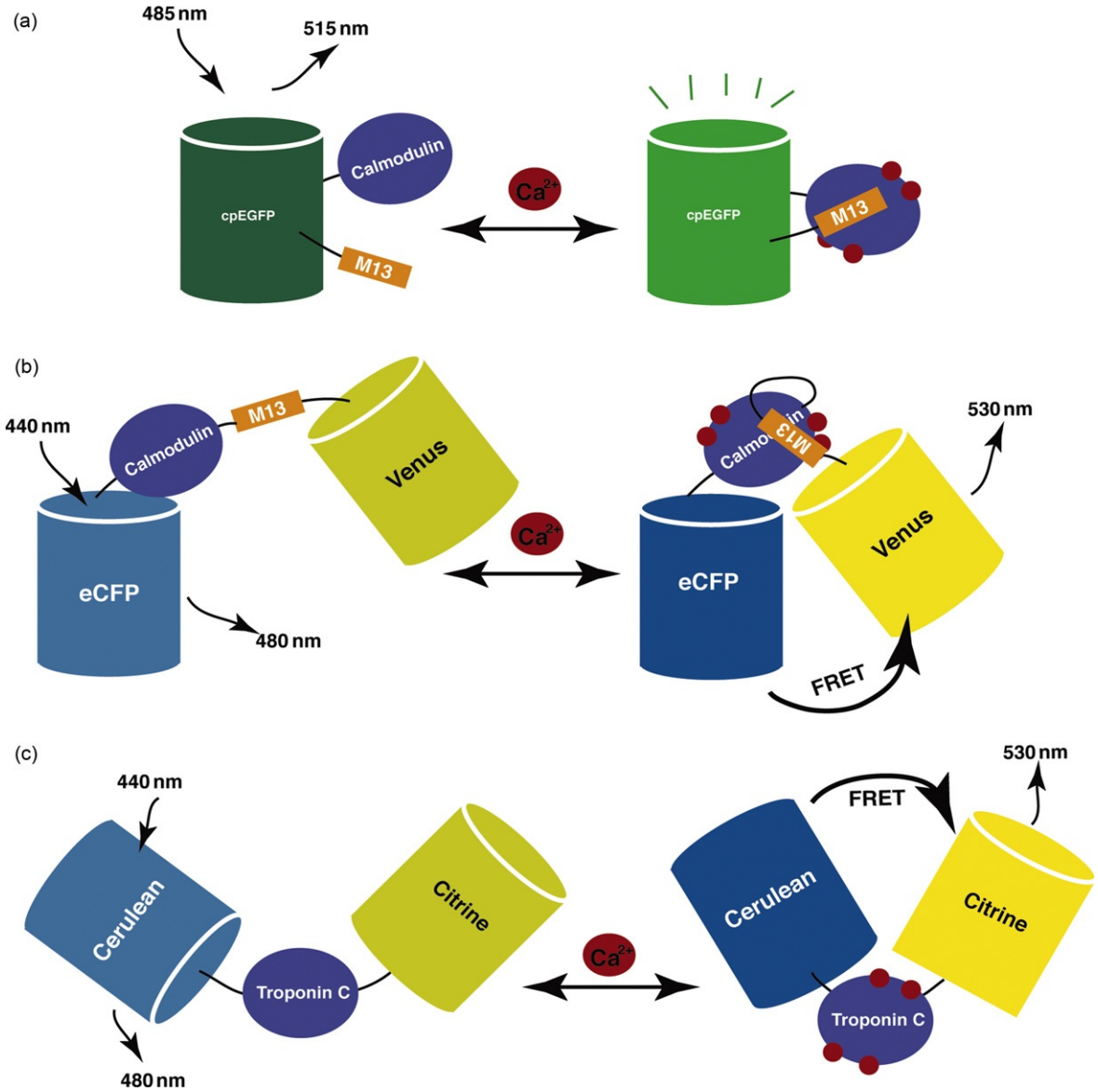

Fig. 1. Schematic representation of the three major GECI classes. GECIs are based either on florescence intensity changes of circularly permuted single FPs (a) or changes in Förster resonance energy transfer (FRET) efficiency between two FPs (b, c). (a) Schematic of the GCaMP-type sensing mechanism. Upon calcium binding, conformational changes in the CaM/M13 complex induce fluorescence changes in the circularly permuted GFP. (b) The Cameleon family of FRET-based GECIs. A calcium-dependent increase in FRET between a CFP and YFP FRET pair is coupled to the binding of calmodulin to the M13 peptide. (c) Troponin C-based FRET GECIs. Binding of calcium to troponin C induces conformational changes and an increase in FRET between CFP and YFP.

mammalian skeletal/cardiac muscle myosin light chain kinase (skMLCK) M13 peptide, came in blue/green and cyan/yellow ("Yellow Cameleon" or "YC") combinations, and had improved fluorescence response relative to FIP-CB_{SM} (Miyawaki et al., 1997). Intriguingly, all Cameleon sequences appear to contain the inadvertent mutation Asp64Tyr, which is a Ca^{2+}-chelating residue in the second EF hand. It is not known what effect this has on their binding affinity, kinetics, or specificity. Since their first publication, the Cameleon family of GECIs has been incrementally improved in terms of FRET signal change, calcium affinity, pH stability, and folding efficiency (for a review, see Palmer et al., 2011). Of note, rational and computational redesign of the CaM/M13 interface diversified the family of Cameleons (D1 (Palmer et al., 2004) was designed by inspection from skMLCK/CaM; D2, D3, and D4 (Palmer et al., 2006) were computationally designed from avian smMLCK/CaM; the Gln-to-Asn mutation in FIP-CB_{SM} was not included; however, a different inadvertent conservative mutation, arginine to lysine, was). These diversified Cameleons exhibit a range of Ca^{2+}-binding affinities and FRET changes and show decreased binding to CaM *in vitro* (Palmer et al., 2006). Whether this translates into decreased interference with CaM signaling pathways *in situ* is not known. It is also impossible to deconvolve the effects of the computational CaM/M13 bump/hole designs of D2, D3, and D4 from the change from mammalian skMLCK to avian smMLCK.

Several of these Cameleon variants have found wide utility in neuroscience. The interface-redesigned sensor D3cpVenus (D3cpV) has been used to detect single APs in organotypic mouse brain slice and *in vivo* in layer 2/3 somatosensory cortical neurons (Wallace et al., 2008). Recently, another Cameleon variant, YC3.60 (Nagai et al., 2004), has been reported to allow *in vivo* detection of single APs with a sensitivity comparable to D3cpV, but with faster kinetics and minimal saturation up to 10 APs (Lütcke et al., 2010). Recently, a very high-affinity variant of YC3.60 (YC-Nano) was shown to detect subtle Ca^{2+} transients associated with spontaneous motor activity in zebrafish embryos (Horikawa et al., 2010), as well as to differentiate resting [Ca^{2+}] levels in different cell types.

The other major two-FP GECI family utilizes the skeletal/cardiac muscle Ca^{2+}-binding protein TnC, instead of CaM. CaM is a ubiquitous intracellular signaling molecule, whereas TnC has historically been considered specific to muscle cells. The current variant, TN-XXL, has been used for chronic *in vivo* activity imaging in mouse and fly (Heim et al., 2007; Reiff et al., 2010). It is not known to what extent TnC-based sensors are truly "orthogonal" to endogenous neuronal signaling mechanisms, since other studies (Aubin-Horth et al., 2005; Fine et al., 1975; Roisen et al., 1983) suggest that TnC may be expressed at high levels in neurons, particularly during development (Schevzov et al., 1997). In mouse brain, overexpression produced a phenotype similar to GCaMP3 and D3cpV (Tian et al., 2009).

Single-FP GECIs include pericam (Nagai et al., 2001), camgaroo (Baird et al., 1999), and GCaMPs. The GCaMP scaffold consists of a circularly permuted green fluorescent protein (cpGFP) with CaM and the M13 peptide (the identical smMLCK as in FIP-CB_{SM}, including the inadvertent Gln-to-Asn mutation) linked to its C- and N-termini, respectively (Nakai et al., 2001). Pericam has a similar architecture to GCaMPs; camgaroo consists of CaM inserted into a yellow FP. Among single-FP GECIs, the GCaMP family has been iteratively optimized and achieved the broadest usage across multiple model organisms. A summary of the historical development of the GCaMP family is shown in Fig. 2.

The first major improvement made to the GCaMP scaffold was the incorporation of GFP thermal stability mutations, which led to the development of GCaMP1.6 (Ohkura et al., 2005). Subsequent random mutagenesis produced the brighter variant GCaMP2 (Diez-Garcia

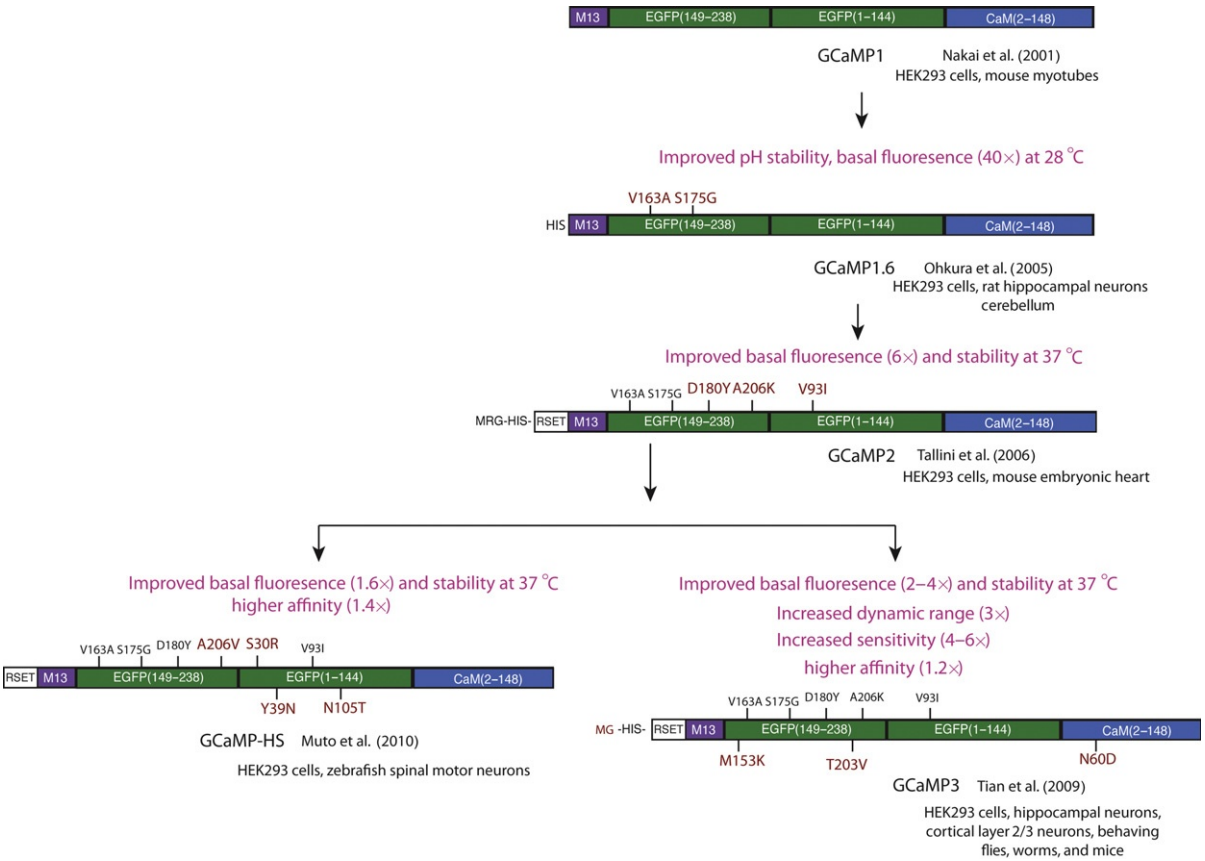

Fig. 2. Summary of the historical development of the GCaMP family. GCaMP family has been iteratively optimized and achieved the broadest usage across multiple model organisms.

et al., 2005; Tallini et al., 2006). GCaMP2 has been used for *in vivo* imaging across multiple model organisms (Chalasani et al., 2007; Diez-Garcia et al., 2005; Hasan et al., 2004, 2008). GCaMP2 has been further optimized by at least three different groups, resulting in GCaMP-HS (Muto et al., 2011) and GCaMP4.1 (Shindo et al., 2010), Case12 and Case16 (Souslova et al., 2007), and GCaMP3 (Tian et al., 2009). A direct comparison of these GCaMPs in terms of their brightness and signal change in neurons has not been performed. GCaMP-HS includes a subset of the "superfolder GFP" mutations (Pedelacq et al., 2006), apparently resulting in increased stability and signal change in zebrafish spinal motor neurons (Muto et al., 2011). Imaging in *Xenopus* embryos has been reported with "GCaMP4.1" (Shindo et al., 2010), although the mutations and/or improvements have not been published. Case12 and Case16 encode a mutation Thr203Phe (near the chromophore); Case16 has an additional Thr145Ser mutation in the second linker (connecting cpGFP to CaM). Both Case sensors showed improvement in *in vitro* response compared to GCaMP2. Case12 has been used to report calcium transients in astrocytes *in vivo* (Gourine et al., 2010), although no *in situ* responses of either Case12 or Case16 have been reported in neurons.

We engineered GCaMP3 from GCaMP2 by a combination of structure-guided design and library screening (Tian et al., 2009). GCaMP3 has increased brightness, Ca^{2+} affinity, and protein stability relative to GCaMP2, and robustly detects single APs in acute mouse brain slice (Tian et al., 2009). This translates into reliable detection of ~3 APs in motor cortex (M1) of an awake, behaving mouse (Tian et al., 2009). The improved properties of GCaMP3 have allowed new types of *in vivo* neural imaging applications in multiple model organisms. In mice, GCaMP3 has been used to image hippocampal place fields during virtual navigation (Dombeck et al., 2010), whisker deflection-induced responses in somatosensory cortex (Mittmann et al., 2011; O'Connor et al., 2010), and light responses of targeted cell populations in retinal explant (Borghuis et al., 2011). In *Drosophila*, GCaMP3 has been used to follow mechanosensory neurons during larval locomotion (Cheng et al., 2010), quantify horizontal-system neural activation in walking adults (Chiappe et al., 2010; Seelig et al., 2010), and map the composition of a pheromone circuit (Ruta et al., 2010). In zebrafish larvae, GCaMP3 facilitated the mapping of a tectal circuit underlying visual discrimination of object size (Del Bene et al., 2010).

Most important, GCaMP3 has made it possible to repeatedly image large neuronal populations over months in mouse M1 (Tian et al., 2009), which has facilitated investigation of learning-mediated changes in neural ensemble representations (D. Huber and K. Svoboda, personal communication). Long-term expression has evinced no apparent behavioral phenotype in model organisms, unlike other GECIs in *Caenorhabditis elegans* (Tian et al., 2009). Extremely high levels of sensor (e.g., at the site of viral injection or *in utero* electroporation) can, however, give rise to an optical correlate for the GCaMP3-induced "cytomorbid" cellular phenotype, in which cells become brightly fluorescent in both cytosol and nucleus, and less excitable (Borghuis et al., 2011; Tian et al., 2009). Similar results were observed with other GECIs such as D3cpV and TN-XXL (Tian et al., 2009). The mechanistic details of this cytotoxicity are not clear; further study will reveal to what extent Ca^{2+} buffering and CaM signaling pathway disruption are implicated, and whether next-generation indicators may alleviate these concerns.

The current set of state-of-the-art GECIs encompasses the single-wavelength indicator, GCaMP3, and the FRET sensors, D3cpV, TN-XXL, and YC3.60. We systematically compared the first three of these in acute mouse brain slice (Tian et al., 2009), with a number of parameters summarized in Table 1. The exact selection of GECI for a given application depends on a number of factors, regarding both indicator properties and experimental constraints. In the next sections, we discuss the factors that need to be taken into consideration in both GECI engineering and application.

Case study: Rational design and systematic screening of GCaMP3

To develop GECIs with properties optimized for a particular application, the appropriate combination of intrinsic GECI parameters should be matched to the extrinsic factors of the system studied. Intrinsic GECI parameters include sensor affinity, kinetics, dynamic range, brightness, expression level, fluorescence properties, and independence from endogenous interference (for recent reviews, see Hires et al., 2008; Tian et al., 2011). Extrinsic parameters include the size, speed, time-course, and frequency of calcium transients, and basal $[Ca^{2+}]$ of the target cell type. Here, using GCaMP3 as an example, we discuss the principles we followed and lessons we learned in improving the GCaMP protein for *in vivo* neurophysiology. We performed structure-guided and library-based protein engineering of the parent scaffold GCaMP2 to optimize each of the following parameters: basal fluorescence intensity, protein stability, dynamic range, and calcium affinity/kinetics.

Table 1. Properties of state-of-the-art GECIs in mouse

In vitro (acute mouse brain slice)							
	$\Delta R/R$, $\Delta F/F$ (%)[a]		Kinetics[a] rise time decay time		Photostability (% fluorescence after 30-min imaging)	*In vivo*	References
Indicators	1 AP	40 AP	(ms)	(ms)			
D3cpV	5±3	40±20	110±30	9500±3400	59 CFP, 84 YFP	Single-spike detection (5% $\Delta R/R$)	Tian et al. (2009), Wallace et al. (2008)
TN-XXL	4±2	50±10	80±20	1600±600	36 CFP, 70 YFP	N/A	Tian et al. (2009)
GCaMP3	14±3	500± 200	100±30	650±200	109 GFP	2–3 AP detection (12–20% $\Delta F/F$), linear up to 20 APs	Tian et al. (2009)
YC3.60	6±0.3	N/A	N/A	800±60	N/A	Single-spike detection (2% $\Delta R/R$), minimal saturation to 10 AP	Lütcke et al. (2010)

[a]Mean±s.d.

The crystal structures of GCaMP2 in both the Ca^{2+}-free and Ca^{2+}-saturated states provide insights into the molecular mechanism of calcium sensing (Akerboom et al., 2009; Wang et al., 2008) and form the basis for rational library design. In the Ca^{2+}-free (apo) structure, much of CaM and the M13 peptide are disordered, suggesting a large amount of flexibility between the M13, cpGFP, and CaM sensor components. In the Ca^{2+}-saturated state, GCaMP2 crystallizes as both a monomer and a dimer, but size-exclusion chromatography experiments suggest that the monomeric form predominates at intracellular concentrations of GCaMP (~10μM) (Akerboom et al., 2009; Hires et al., 2008). The monomer structure shows considerable domain movement and conformational differences compared to the apo-state of GCaMP; CaM is tightly wrapped around M13 and packs against the GFP barrel opening created by circular permutation (Akerboom et al., 2009). This induces a reorganization of the GFP chromophore chemical environment, resulting in a decrease in solvent access and a downward shift of the tyrosyl hydroxyl pK_a that moves the equilibrium toward the deprotonated, bright state at physiological pH. Other factors such as alteration of dynamics influencing excited state lifetime or extinction coefficient are also possible but are not directly addressed by the available biophysical data. An important result of the crystal structures was to delineate the interface between CaM and cpGFP such that these positions could be targeted for mutagenic screening. To increase the dynamic range of GCaMP2, we selected a group of amino acids in close proximity to the chromophore in both the apo and the Ca^{2+}-bound (sat) states for mutagenesis. To increase protein stability at physiological temperatures, we tuned the expression and turnover of GCaMP2 by changing the N-terminally encoded proteasomal degradation sequence; we also mutated positions known to regulate GFP thermodynamic stability. Finally, we made libraries of the Ca^{2+}-binding EF hands and the CaM/M13 binding surface to screen for mutants with higher Ca^{2+} affinity.

Our initial screens were performed in *Escherichia coli* lysates. However, we found that correlation between sensor performance in bacterial lysate or purified protein, and that in slice,

was relatively low; the GCaMP2-LIA mutant is an example of this (Tian et al., 2009). As each system or cell type has a unique calcium signaling toolkit and may handle GECIs and Ca^{2+} differently, we first sought to establish a standardized screening paradigm balancing throughput with downstream predictability. For developmental efficiency, such an initial testing system should allow screening for brightness, calcium sensitivity, dynamic range, and kinetics with decent throughput. It should also capture as many aspects of intact preparations (e.g., calcium buffering and cytotoxicity) as possible, allowing better prediction of GECI performance in more challenging environments. The method we settled on uses agonized endogenous G-protein-coupled receptors in cultured mammalian cells to create synthetic Ca^{2+} transients lasting tens of seconds (Tian et al., 2009). The biggest disadvantage of this method is that the use of alternative cell types may obscure the dynamic aspects of Ca^{2+} signaling unique to neuronal morphology and physiology. As an alternative, testing GECI performance in dissociated neuronal cultures coupled to field potential stimuli may provide a better platform (Janelia Farm GECI Project, unpublished data). Even cultured neurons, however, may differ dramatically from an *in vivo* setting (e.g., disrupted network connectivity), and more intact preparations are invariably required to validate candidate hits.

Following an initial high-throughput screen, a small number of high-quality sensors can be further characterized in cortical pyramidal neurons in acute slice with simultaneous two-photon imaging and electrophysiology (Mao et al., 2008; Tian et al., 2009). Imaging GECI responses to evoked back-propagating APs is the most reliable way to assess relevant sensor kinetics and signal change, and captures many aspects of *in vivo* functional imaging (e.g., possible long-term expression and developmental effects), while allowing a moderate throughput (together with *in utero* electroporation). To optimize GCaMP signal, the laser is typically tuned to 910 nm, although the interval 900–1000 nm all works well for excitation. The typical imaging configuration is line-scan mode (500 Hz) across the apical dendrite, 20–50 μm from the base of the neuron (Tian et al., 2009). We triggered defined numbers of APs at specific intervals with intermittent short depolarizing pulses (Hendel et al., 2008). Alternatively, neurons can be depolarized by continuous current injection from a patch pipette (Pologruto et al., 2004).

Finally, the performance of the best candidates needs to be confirmed in an *in vivo* preparation, with such complicating factors as sample access, imaging depth, motion artifacts, and hemodynamics. To do this, we expressed a few of the best GCaMPs postnatally in neurons of M1 by adeno-associated virus (AAV)-mediated gene transfer. We observed uniform, bright labeling of layer 2/3 pyramidal cells, of cell bodies and neurites alike. We performed simultaneous electrophysiological recordings and two-photon imaging via a loose seal cell-attached configuration. We observed robust fluorescent transients following spontaneous, sensory-related, or AP-evoked calcium transients (Tian et al., 2009). Responses were imaged for several months, with no apparent decline in sensor performance or neuronal morphology. Of course, each system will have unique considerations; comparison of new GECIs across a set of model organisms (e.g., *C. elegans*, *Drosophila*, mouse, zebrafish) will best give a sense of an indicator's strengths and weaknesses.

In addition to ensuring that a GECI faithfully reports neural activity, it is equally important to evaluate the potential endogenous interference in cells caused by GECI expression. Every GECI by definition will sequester Ca^{2+}. Expressing high levels of indicator to achieve good SNR may magnify such calcium buffering. GECIs composed of endogenous Ca^{2+}-binding proteins run the further risk of activating cellular signal transduction pathways. These two (at least) mechanisms of endogenous interference may lead to perturbations in cell physiology, synaptic and circuit activity, and ultimately behavior. A variety of biochemical and physiological approaches, such as

immunohistochemistry and patch clamping, can be used to evaluate neuronal morphology and electrophysiological parameters (e.g., R_m, C_m, E_m) in GECI-positive and -negative cells. At the network level, laser-scanning photostimulation circuit mapping (Petreanu et al., 2007, 2009) can test for changes in synaptic properties and connectivity patterns (Tian et al., 2009). In the end, a robust behavioral paradigm is required to test for possible perturbations to the system and to the model organism as a whole.

Choosing the best GECI for a given application

For end users, choosing the most appropriate GECI at the start of a project is paramount, since experimental optimization requires significant investments in time and resources. GECI selection will also influence many other choices, for example, light source, filters, camera, image analysis algorithms, etc. A good rule of thumb is to characterize several GECIs in the context of a specific application, as they each have different strengths and weaknesses. Here, we discuss several practical criteria that users may wish to consider.

Two- versus one-FP GECIs

In general, FRET-based two-FP sensors have higher basal brightness (since they are typically based on intact FPs) and are less sensitive to motion artifacts or expression level differences (due to ratioing of the donor and acceptor fluorescence). In addition, FRET-based GECIs are better suited for applications in which precise quantification of $[Ca^{2+}]$ is desired. However, they require simultaneous measurement of fluorescence in two channels, slowing down measurement, compounding errors, and consuming large spectral bandwidth. Differential photobleaching, bleed-through between donor and acceptor FPs, and other artifacts may confound measurement and analysis (Piston and Kremers, 2007).

Intensity-based single-FP GECIs usually have superior dynamic range, kinetics, SNR, and photostability when compared to FRET-based GECIs (Table 1) (Mao et al., 2008; Tian et al., 2009). The smaller size of single-FP GECIs makes them more suitable for protein fusions to target specific cellular compartments and for viral payloading. They may also be used in conjunction with other labels or probes for multicolor imaging, since the spectral bandwidth is preserved. All FPs are intrinsically pH-sensitive, and this will affect both one- and two-FP GECIs. pH sensitivity may be exacerbated for one-FP GECIs based on circularly permuted FPs. A comparison between these two GECI classes is shown in Fig. 3.

Calcium affinity, kinetics, and dynamic range

The fluorescence response of a GECI to calcium transients is critically dependent on its affinity, kinetics, and dynamic range (Hires et al., 2008). To achieve optimal SNR, it is essential to match these parameters with the calcium dynamics of the system under study. In addition, a linear relationship between fluorescence response and target stimulus facilitates quantitative measurement of calcium transients (Sasaki et al., 2008). Cell-to-cell variability of GECI responses (e.g., see Fig. 7 in Borghuis et al., 2011; Fig. 6 in Tian et al., 2009) may complicate quantitation of responses across cell populations. For events inducing small calcium transients, such as sparse APs, a GECI with high affinity and fast on-kinetics is preferred (Hires et al., 2008). A slow decay rate (off-kinetics) may facilitate signaling integration, leading to better detection of lower or sparse APs (Wallace et al., 2008) but will confound interpretation of spike trains with high frequency. Indicator decay rates are not always the limiting factor for observed kinetics. For instance, dendritic GCaMP3 transients were roughly twice as fast as somatic responses in the same retinal ganglion cell (Borghuis et al., 2011). For events with large calcium transients, such as

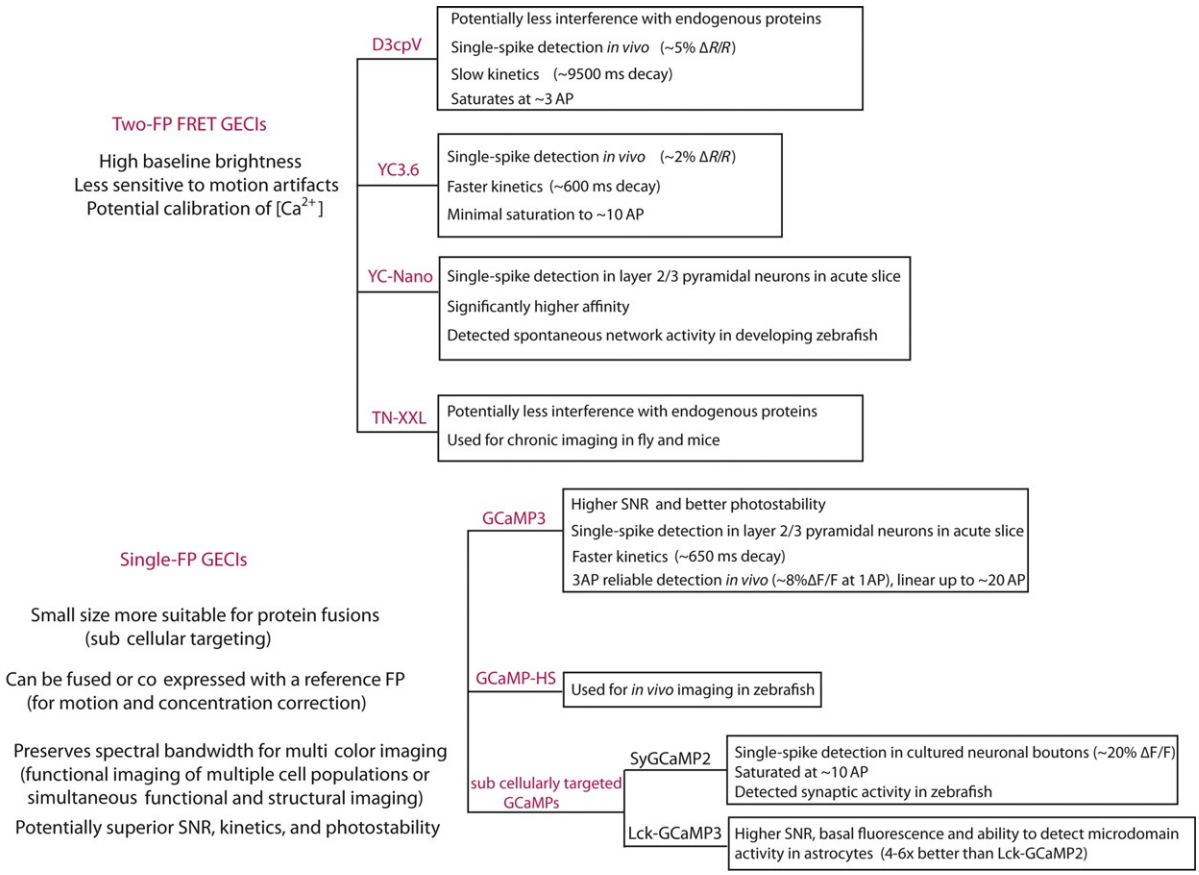

Fig. 3. A comparison between two-FP- or single-FP-based GECI classes.

in fast-spiking neurons, a low-affinity sensor will provide a greater effective dynamic range.

GECI expression level

The expression level of a GECI influences its performance in cells and organisms, in a complex manner. Very low GECI expression will preclude even sensor visualization. As [GECI] increases, the number of photons detected increases, but the amount of buffered Ca^{2+} will increase, which decreases $\Delta F/F$. These two opposing effects give rise to an "inverted U"-shaped plot for SNR as a function of [GECI], with a simulated optimum of ~5–20 μM for best SNR (Hires et al., 2008). In addition, higher [GECI] will tend to spread transients out (Helmchen et al., 1996), confounding kinetic analysis. On the other hand, it will facilitate imaging with lower laser power and/or shorter exposure times; this favorably impacts imaging speed and phototoxicity. In addition, GECI components (e.g., CaM, M13pep) may be sequestered by endogenous proteins, thus resulting in nonfunctional indicators that can increase background fluorescence (Hasan et al., 2004; Heim and Griesbeck, 2004; Tian et al., 2009). Such endogenous interference may also

perturb cell-signaling pathways and lead to behavioral phenotypes as discussed above (Tian et al., 2009).

Balancing all these effects, we find that it is usually best to shoot for the lowest GECI expression level that allows imaging with tolerably low laser power. To accomplish this, users may wish to explore multiple promoters, regulatory sequences, and transduction methods (e.g., different viral serotypes, electroporation techniques, or transgenic lines). Following both *in utero* electroporation of a *CAG* promoter construct and AAV infection with a *synapsin-1* promoter, we found [GCaMP3] levels to be on the order of ~10 μM (Hires et al., 2008; Tian et al., 2009, 2011). This falls in the predicted range with high SNR with low cyto- and phototoxicity.

Subcellular targeting

One of the advantages of GECIs over small molecules is the ability to target them to specific subcellular locations. GECIs can fill some cellular compartments, such as dendrites and axons, without fusion to targeting peptides or proteins. For instance, expressing GCaMP3 in cortical layer 5 neurons (via stereotactic viral injection) allowed for apical dendritic imaging far away (~600–800 μm) from their somas of origin (Mittmann et al., 2011). Alternatively, GECIs can be targeted to specific subcellular compartments via protein fusions or signaling peptides. Different subcellular compartments experience unique Ca^{2+} fluxes; thus matching GECI properties to the calcium dynamics in the target environment is essential. For example, a low-affinity GECI may be less useful for probing small calcium transients in the cytosol, but highly effective at measuring large calcium transients in the endoplasmic reticulum and mitochondria (Miyawaki et al., 1997). Targeting a GECI to subcellular locations where calcium transients tend to be larger, such as synaptic terminals (Dreosti et al., 2009) or near the plasma membrane (Shigetomi et al., 2010a,b), can improve SNR without altering the sensor itself. Subcellular targeting may, however, negatively impact photostability of the sensor under laser-scanning illumination due to decreased protein mobility (L. Petreanu and K. Svoboda, personal communication). Fusion to essential proteins may also interfere with their evolved functions (T. Ryan, personal communication). Therefore, it is important to consider the impact of such manipulations on both the sensor and its environment before settling on a final targeting strategy.

Imaging neural activity with GECIs *in vivo*

Through iterative cycles of optimization, GECIs have been improved to the point that they are useful for *in vivo* neuronal imaging. State-of-the-art GECIs, such as D3cpV, YC3.60, YC-Nano, GCaMP-HS, and GCaMP3, have been widely used to report neural activity in living zebrafish (Muto et al., 2011), worms (Tian et al., 2009), flies (Cheng et al., 2010; Chiappe et al., 2010; Heim et al., 2007; Seelig et al., 2010; Tian et al., 2009), and mice (Dombeck et al., 2010; Lütcke et al., 2010; Mittmann et al., 2011; O'Connor et al., 2010; Tian et al., 2009; Wallace et al., 2008).

To make imaging data meaningful for quantitative neural activity measurements, calibration of GECI responses to ground truth measurements of spike trains in a representative set of neurons is necessary. In the mammalian brain, such calibration can be performed via cell-attached recording of spontaneous or sensory-evoked APs (Tian et al., 2009). Sensor response may vary from cell to cell, presumably due to variations in expression level, which can complicate interpretation. Such cell-to-cell variability is most apparent using *in utero* electroporation and to a lesser extent viral transduction. Transgenics, especially knock-ins, may alleviate this variability to some degree. Image processing is a necessary but tedious step, as signals must be assigned (segmented) to specific cells. This is inherently

difficult and is further complicated by low probe SNR, dense labeling, motion artifacts, neuropil signal, probe photobleaching, tissue autofluorescence, hemodynamics, light scattering, artifacts from probe cytotoxicity, illumination phototoxicity, etc. A number of algorithmic improvements have been recently published (Greenberg and Kerr, 2009; Mukamel et al., 2009; Valmianski et al., 2010). Following segmentation, firing rate changes can be extracted from imaging traces via deconvolution (Yaksi and Friedrich, 2006), machine learning (Sasaki et al., 2008; D. Huber, D. Gutnisky, and K. Svoboda, personal communication), or Monte Carlo simulation (Vogelstein et al., 2009), among others.

The noise level *in vivo* greatly challenges the SNR of the sensor, which depends on the imaging configuration, surgical procedures (e.g., cranial window implantation or skull thinning (Yang et al., 2010), probe brightness, expression level, and imaging depth, among many other parameters. For reliably detecting sparse AP firing *in vivo*, especially single APs, further GECI engineering will be necessary. The kinetics of currently available GECIs is too slow to reconstruct high-frequency firing events. Potential cytotoxicity caused by long-term, high-level GECI expression can also make chronic *in vivo* imaging difficult. On the other hand, low-level GECI expression not only compromises SNR but also requires longer exposure times or higher excitation intensity, which can lead to sensor bleaching or tissue damage. To balance high SNR with minimal cytotoxicity, expression cassettes that are inducible and reversible or that hold [GECI] steady for long periods of time would facilitate signal calibration and further reduce toxicity concerns in chronic imaging. Finally, development of optics allowing faster, deeper, and higher-resolution imaging will greatly increase GECI utility. Recently, the applications of adaptive optics to two-photon microscopy to correct aberrations (Ji et al., 2010) and regenerative amplification to increase light penetration (Mittmann et al., 2011) have significantly increased the depth at which imaging may be reliably performed.

To target GECIs to genetically defined neuronal populations, a variety of genetic methods can be used. For example, transgenic lines expressing "drivers" (e.g., Cre recombinase or the Gal4 transcriptional activator) in specific cell types (with tissue-specific promoters) can be combined with "reporter" strains or viruses containing Cre- or Gal4/UAS-dependent GECIs (for review of such two-component systems, see Luo et al., 2008; Simpson, 2009). Large numbers of *Drosophila* Gal4 lines and Cre mice are currently available. Alternatively, a small but growing number of *cis*-regulatory elements (e.g., *synapsin-1*, *CaMKIIα*) can target transgenes delivered by viral infection or electroporation, even in non-genetic-model organisms. Through the combination of promoter selection and inherent viral serotype tropism, AAV vectors enable regional expression via local viral injection and have been broadly used to deliver sensors or other molecular tools to cell types of interest for mapping, monitoring, and manipulating neural circuitry (Betley and Sternson, 2011; Borghuis et al., 2011).

Expression of genetically encoded sensors may potentially perturb the physiology of the system studied, which is one of the major challenges for *in vivo* imaging, especially for applications where chronic imaging is required, for example, learning or disease progression. To facilitate signal calibration, protein sensors should be expressed at steady-state levels in individual neurons for long periods of time without altering physiology. At the same time, sensor performance should be constant to enable quantitative analysis. Optimizing sensors for *in vivo* application is difficult, although progress has been made (Tian et al., 2009). For each application, the timing and magnitude of sensor expression should be optimized to balance signal and cytotoxicity, by testing multiple promoters, regulatory sequences, and transduction methods (e.g., screening different viral serotypes, integration methods, copy number, etc.). Careful experiments are required to determine the effects of long-term GECI expression on both single-cell physiology and circuit function.

Outlook

The primary focus of current GECI engineering efforts is to further increase the SNR for robust detection of low firing rates (ideally single APs) in a variety of systems *in vivo*. Engineering high-affinity sensors for probing small stimuli while preserving fast kinetics is challenging (Mank et al., 2006). Further optimization of the GCaMP, Cameleon, and TnC sensor formats will undoubtedly improve signals in the short term. Alternatively, novel GECI scaffolds, with different (perhaps faster) calcium-binding proteins, may be employed to overcome this limitation.

Additionally, expanding the color spectrum of GECIs, particularly into the red and near-infrared, will open up many new applications in neuroscience, due to deeper tissue penetration, decreased autofluorescence, and less phototoxicity (Shcherbo et al., 2010). Also, many transgenic mouse lines already contain GFP (or equivalent), which precludes easy use of current GECIs for functional imaging. Red-shifted single-FP GECIs would not only facilitate deep imaging but also enable functional imaging from multiple cell populations and/or subcellular compartments, and make it easier to use with light-gated proteins such as channelrhodopsin-2 (Zhao et al., 2011). With the constant improvement of red and far-red FPs (Lin et al., 2009; Shcherbo et al., 2009, 2010; Shu et al., 2009), viable red-shifted GECIs should be possible.

The next generation of neural activity probes will be faster and more sensitive than the current one. It will also feature different colors of GECIs that can be used in concert. Mechanisms of GECI cytotoxicity must be elucidated; more "bio-orthogonal" sensor elements may help with this. Concomitant with this, improving indicator SNR will enable expression at lower levels, which reduces concerns. Other indicator improvements will include photoactivatable versions that can be turned on in selected populations and those that integrate [Ca^{2+}] over time. A defined toolkit of expression systems, such as transgenic mice and a library of viral serotype–promoter combinations, will further facilitate technology uptake. These advancements, together with improvement in the areas of lasers, cameras, imaging processing and deconvolution algorithms, and computation, will make long-term, high-resolution *in vivo* functional imaging in large, defined cell populations a reality.

Reagent availability

GCaMP3 plasmid DNA (*CMV* promoter for expression in mammalian cells) is available from Addgene (addgene.org): #22692. A membrane-fused version (Lck) is also available: #26974. Live AAV virus and pAAV constructs for both GCaMP3 and a Cre-dependent FLEX-GCaMP3 are available from the U Penn Vector Core, driven by a *synapsin-1* promoter (http://www.med.upenn.edu/gtp/vectorcore/Catalogue.shtml). *Drosophila* strains expressing GCaMP3 under *UAS* control are available from the Bloomington Stock Collection (#32116, #32234–32237; inserts are available on the X, 2L, and 3L chromosomes). A Cre-dependent GCaMP3 reporter mouse (*ROSA26* locus; *CAG* promoter) has been deposited at Jackson Labs (#014538). The Janelia Farm GECI Project continues to develop the GCaMP scaffold, as well as other GECIs. Information on the Project can be found at http://www.janelia.org/team-project/geci-project.

Note added in proof

Recently, blue- and red- shifted single-FP GECIs have been demonstrated (Zhao et al., 2011).

References

Akerboom, J., Rivera, J. D., Guilbe, M. M., Malave, E. C., Hernandez, H. H., Tian, L., et al. (2009). Crystal structures of the GCaMP calcium sensor reveal the mechanism of fluorescence signal change and aid rational design. *The Journal of Biological Chemistry*, *284*, 6455–6464.

Aubin-Horth, N., Landry, C. R., Letcher, B. H., & Hofmann, H. A. (2005). Alternative life histories shape brain gene expression profiles in males of the same population. *Proceedings of the Royal Society B*, *272*, 1655–1662.

Baird, G. S., Zacharias, D. A., & Tsien, R. Y. (1999). Circular permutation and receptor insertion within green fluorescent proteins. *Proceedings of the National Academy of Sciences of the United States of America*, *96*, 11241–11246.

Betley, J. N., & Sternson, S. M. (2011). Adeno-associated viral vectors for mapping, monitoring, and manipulating neural circuits. *Human Gene Therapy*, *22*, 669–677.

Borghuis, B. G., Tian, L., Xu, Y., Nikonov, S. S., Vardi, N., Zemelman, B. V., et al. (2011). Imaging light responses of targeted neuron populations in the rodent retina. *The Journal of Neuroscience*, *31*, 2855–2867.

Chalasani, S. H., Chronis, N., Tsunozaki, M., Gray, J. M., Ramot, D., Goodman, M. B., et al. (2007). Dissecting a circuit for olfactory behaviour in Caenorhabditis elegans. *Nature*, *450*, 63–70.

Cheng, L. E., Song, W., Looger, L. L., Jan, L. Y., & Jan, Y. N. (2010). The role of the TRP channel NompC in Drosophila larval and adult locomotion. *Neuron*, *67*, 373–380.

Chiappe, M. E., Seelig, J. D., Reiser, M. B., & Jayaraman, V. (2010). Walking modulates speed sensitivity in Drosophila motion vision. *Current Biology*, *20*, 1470–1475.

Del Bene, F., Wyart, C., Robles, E., Tran, A., Looger, L., Scott, E. K., et al. (2010). Filtering of visual information in the tectum by an identified neural circuit. *Science*, *330*, 669–673.

Diez-Garcia, J., Matsushita, S., Mutoh, H., Nakai, J., Ohkura, M., Yokoyama, J., et al. (2005). Activation of cerebellar parallel fibers monitored in transgenic mice expressing a fluorescent Ca2+ indicator protein. *The European Journal of Neuroscience*, *22*, 627–635.

Dombeck, D. A., Harvey, C. D., Tian, L., Looger, L. L., & Tank, D. W. (2010). Functional imaging of hippocampal place cells at cellular resolution during virtual navigation. *Nature Neuroscience*, *13*, 1433–1440.

Dreosti, E., Odermatt, B., Dorostkar, M. M., & Lagnado, L. (2009). A genetically encoded reporter of synaptic activity in vivo. *Nature Methods*, *6*, 883–889.

Fine, R., Lehman, W., Head, J., & Blitz, A. (1975). Troponin C in brain. *Nature*, *258*, 260–267.

Gourine, A. V., Kasymov, V., Marina, N., Tang, F., Figueiredo, M. F., Lane, S., et al. (2010). Astrocytes control breathing through pH-dependent release of ATP. *Science*, *329*, 571–575.

Greenberg, D. S., & Kerr, J. N. (2009). Automated correction of fast motion artifacts for two-photon imaging of awake animals. *Journal of Neuroscience Methods*, *176*, 1–15.

Hasan, M. T., Friedrich, R. W., Euler, T., Larkum, M. E., Giese, G., Both, M., et al. (2004). Functional fluorescent Ca2+ indicator proteins in transgenic mice under TET control. *PLoS Biology*, *2*, e163.

He, J., Ma, L., Kim, S., Nakai, J., & Yu, C. R. (2008). Encoding gender and individual information in the mouse vomeronasal organ. *Science*, *320*, 535–538.

Heim, N., Garaschuk, O., Friedrich, M. W., Mank, M., Milos, R. I., Kovalchuk, Y., et al. (2007). Improved calcium imaging in transgenic mice expressing a troponin C-based biosensor. *Nature Methods*, *4*, 127–129.

Heim, N., & Griesbeck, O. (2004). Genetically encoded indicators of cellular calcium dynamics based on troponin C and green fluorescent protein. *The Journal of Biological Chemistry*, *279*, 14280–14286.

Helmchen, F., Imoto, K., & Sakmann, B. (1996). Ca2+ buffering and action potential-evoked Ca2+ signaling in dendrites of pyramidal neurons. *Biophysical Journal*, *70*, 1069–1081.

Hendel, T., Mank, M., Schnell, B., Griesbeck, O., Borst, A., & Reiff, D. F. (2008). Fluorescence changes of genetic calcium indicators and OGB-1 correlated with neural activity and calcium in vivo and in vitro. *The Journal of Neuroscience*, *28*, 7399–7411.

Hires, S. A., Tian, L., & Looger, L. L. (2008). Reporting neural activity with genetically encoded calcium indicators. *Brain Cell Biology*, *36*, 69–86.

Horikawa, K., Yamada, Y., Matsuda, T., Kobayashi, K., Hashimoto, M., Matsu-ura, T., et al. (2010). Spontaneous network activity visualized by ultrasensitive Ca(2+) indicators, yellow Cameleon-Nano. *Nature Methods*, *7*, 729–732.

Ji, N., Milkie, D. E., & Betzig, E. (2010). Adaptive optics via pupil segmentation for high-resolution imaging in biological tissues. *Nature Methods*, *7*, 141–147.

Lin, M. Z., McKeown, M. R., Ng, H. L., Aguilera, T. A., Shaner, N. C., Campbell, R. E., et al. (2009). Autofluorescent proteins with excitation in the optical window for intravital imaging in mammals. *Chemistry & Biology*, *16*, 1169–1179.

Luo, L., Callaway, E. M., & Svoboda, K. (2008). Genetic dissection of neural circuits. *Neuron*, *57*, 634–660.

Lütcke, H., Murayama, M., Hahn, T., Margolis, D. J., Astori, S., zum Alten Borgloh, S. M., et al. (2010). Optical recording of neuronal activity with a genetically-encoded calcium indicator in anesthetized and freely moving mice. *Frontiers in Neural Circuits*, *4*, 9.

Mank, M., Reiff, D. F., Heim, N., Friedrich, M. W., Borst, A., & Griesbeck, O. (2006). A FRET-based calcium biosensor with fast signal kinetics and high fluorescence change. *Biophysical Journal*, *90*, 1790–1796.

Mao, T., O'Connor, D. H., Scheuss, V., Nakai, J., & Svoboda, K. (2008). Characterization and subcellular targeting of GCaMP-type genetically-encoded calcium indicators. *PLoS One*, *3*, e1796.

Mittmann, W., Wallace, D. J., Czubayko, U., Herb, J. T., Schaefer, A. T., Looger, L. L., et al. (2011). Two-photon calcium imaging of evoked activity from L5 somatosensory neurons in vivo. *Nature Neuroscience*, *14*, 1089–1093.

Miyawaki, A. (2011). Development of probes for cellular functions using fluorescent proteins and fluorescence

resonance energy transfer. *Annual Review of Biochemistry*, *80*, 357–373.

Miyawaki, A., Llopis, J., Heim, R., McCaffery, J. M., Adams, J. A., Ikura, M., et al. (1997). Fluorescent indicators for Ca2+ based on green fluorescent proteins and calmodulin. *Nature*, *388*, 882–887.

Mukamel, E. A., Nimmerjahn, A., & Schnitzer, M. J. (2009). Automated analysis of cellular signals from large-scale calcium imaging data. *Neuron*, *63*, 747–760.

Muto, A., Ohkura, M., Kotani, T., Higashijima, S., Nakai, J., & Kawakami, K. (2011). Genetic visualization with an improved GCaMP calcium indicator reveals spatiotemporal activation of the spinal motor neurons in zebrafish. *Proceedings of the National Academy of Sciences of the United States of America*, *108*, 5425–5430.

Nagai, T., Sawano, A., Park, E. S., & Miyawaki, A. (2001). Circularly permuted green fluorescent proteins engineered to sense Ca2+. *Proceedings of the National Academy of Sciences of the United States of America*, *98*, 3197–3202.

Nagai, T., Yamada, S., Tominaga, T., Ichikawa, M., & Miyawaki, A. (2004). Expanded dynamic range of fluorescent indicators for Ca(2+) by circularly permuted yellow fluorescent proteins. *Proceedings of the National Academy of Sciences of the United States of America*, *101*, 10554–10559.

Nakai, J., Ohkura, M., & Imoto, K. (2001). A high signal-to-noise Ca(2+) probe composed of a single green fluorescent protein. *Nature Biotechnology*, *19*, 137–141.

O'Connor, D. H., Peron, S. P., Huber, D., & Svoboda, K. (2010). Neural activity in barrel cortex underlying vibrissa-based object localization in mice. *Neuron*, *67*, 1048–1061.

Ohkura, M., Matsuzaki, M., Kasai, H., Imoto, K., & Nakai, J. (2005). Genetically encoded bright Ca2+ probe applicable for dynamic Ca2+ imaging of dendritic spines. *Analytical Chemistry*, *77*, 5861–5869.

Palmer, A. E., Giacomello, M., Kortemme, T., Hires, S. A., Lev-Ram, V., Baker, D., et al. (2006). Ca2+ indicators based on computationally redesigned calmodulin-peptide pairs. *Chemical Biology*, *13*, 521–530.

Palmer, A. E., Jin, C., Reed, J. C., & Tsien, R. Y. (2004). Bcl-2-mediated alterations in endoplasmic reticulum Ca2+ analyzed with an improved genetically encoded fluorescent sensor. *Proceedings of the National Academy of Sciences of the United States of America*, *101*, 17404–17409.

Palmer, A. E., Qin, Y., Park, J. G., & McCombs, J. E. (2011). Design and application of genetically encoded biosensors. *Trends in Biotechnology*, *29*, 144–152.

Pedelacq, J. D., Cabantous, S., Tran, T., Terwilliger, T. C., & Waldo, G. S. (2006). Engineering and characterization of a superfolder green fluorescent protein. *Nature Biotechnology*, *24*, 79–88.

Petreanu, L., Huber, D., Sobczyk, A., & Svoboda, K. (2007). Channelrhodopsin-2-assisted circuit mapping of long-range callosal projections. *Nature Neuroscience*, *10*, 663–668.

Petreanu, L., Mao, T., Sternson, S. M., & Svoboda, K. (2009). The subcellular organization of neocortical excitatory connections. *Nature*, *457*, 1142–1145.

Piston, D. W., & Kremers, G. J. (2007). Fluorescent protein FRET: The good, the bad and the ugly. *Trends in Biochemical Sciences*, *32*, 407–414.

Pologruto, T. A., Yasuda, R., & Svoboda, K. (2004). Monitoring neural activity and [Ca2+] with genetically encoded Ca2+ indicators. *The Journal of Neuroscience*, *24*, 9572–9579.

Reiff, D. F., Plett, J., Mank, M., Griesbeck, O., & Borst, A. (2010). Visualizing retinotopic half-wave rectified input to the motion detection circuitry of Drosophila. *Nature Neuroscience*, *13*, 973–978.

Roisen, F. J., Wilson, F. J., Yorke, G., Inczedy-Marcsek, M., & Hirabayashi, T. (1983). Immunohistochemical localization of troponin-C in cultured neurons. *Journal of Muscle Research and Cell Motility*, *4*, 163–175.

Romoser, V. A., Hinkle, P. M., & Persechini, A. (1997). Detection in living cells of Ca2+−dependent changes in the fluorescence emission of an indicator composed of two green fluorescent protein variants linked by a calmodulin-binding sequence. A new class of fluorescent indicators. *Journal of Chemical Biology*, *272*, 13270–13274.

Ruta, V., Datta, S. R., Vasconcelos, M. L., Freeland, J., Looger, L. L., & Axel, R. (2010). A dimorphic pheromone circuit in Drosophila from sensory input to descending output. *Nature*, *468*, 686–690.

Sasaki, T., Takahashi, N., Matsuki, N., & Ikegaya, Y. (2008). Fast and accurate detection of action potentials from somatic calcium fluctuations. *Journal of Neurophysiology*, *100*, 1668–1676.

Scanziani, M., & Hausser, M. (2009). Electrophysiology in the age of light. *Nature*, *461*, 930–939.

Schevzov, G., Gunning, P., Jeffrey, P. L., Temm-Grove, C., Helfman, D. M., Lin, J. J., et al. (1997). Tropomyosin localization reveals distinct populations of microfilaments in neurites and growth cones. *Molecular and Cellular Neurosciences*, *8*, 439–454.

Seelig, J. D., Chiappe, M. E., Lott, G. K., Dutta, A., Osborne, J. E., Reiser, M. B., et al. (2010). Two-photon calcium imaging from head-fixed Drosophila during optomotor walking behavior. *Nature Methods*, *7*, 535–540.

Shcherbo, D., Murphy, C. S., Ermakova, G. V., Solovieva, E. A., Chepurnykh, T. V., Shcheglov, A. S., et al. (2009). Far-red fluorescent tags for protein imaging in living tissues. *The Biochemical Journal*, *418*, 567–574.

Shcherbo, D., Shemiakina, I. I., Ryabova, A. V., Luker, K. E., Schmidt, B. T., Souslova, E. A., et al. (2010). Near-infrared fluorescent proteins. *Nature Methods*, *7*, 827–829.

Shigetomi, E., Kracun, S., & Khakh, B. S. (2010). Monitoring astrocyte calcium microdomains with improved membrane targeted GCaMP reporters. *Neuron Glia Biology*, *16*, 1–9 [Epub ahead of print].

Shigetomi, E., Kracun, S., Sofroniew, M. V., & Khakh, B. S. (2010). A genetically targeted optical sensor to monitor calcium signals in astrocyte processes. *Nature Neuroscience*, *13*, 759–766.

Shindo, A., Hara, Y., Yamamoto, T. S., Ohkura, M., Nakai, J., & Ueno, N. (2010). Tissue-tissue interaction-triggered calcium elevation is required for cell polarization during Xenopus gastrulation. *PLoS One*, *5*, e8897.

Shu, X., Royant, A., Lin, M. Z., Aguilera, T. A., Lev-Ram, V., Steinbach, P. A., et al. (2009). Mammalian expression of infrared fluorescent proteins engineered from a bacterial phytochrome. *Science*, *324*, 804–807.

Simpson, J. H. (2009). Mapping and manipulating neural circuits in the fly brain. *Advances in Genetics*, *65*, 79–143.

Souslova, E. A., Belousov, V. V., Lock, J. G., Stromblad, S., Kasparov, S., Bolshakov, A. P., et al. (2007). Single fluorescent protein-based Ca2+ sensors with increased dynamic range. *BMC Biotechnology*, *7*, 37.

Svoboda, K., & Yasuda, R. (2006). Principles of two-photon excitation microscopy and its applications to neuroscience. *Neuron*, *50*, 823–839.

Tallini, Y. N., Ohkura, M., Choi, B. R., Ji, G., Imoto, K., Doran, R., et al. (2006). Imaging cellular signals in the heart in vivo: Cardiac expression of the high-signal Ca2+ indicator GCaMP2. *Proceedings of the National Academy of Sciences of the United States of America*, *103*, 4753–4758.

Tian, L., Hires, S. A., & Looger, L. L. (2011). Imaging neuronal activity with genetically encoded calcium indicators. In F. Helmchen & A. Konnerth (Eds.), *Imaging in neuroscience: A laboratory manual* (pp. 63–73). Cold Spring Harbor, NY: Cold Spring Harbor Laboratory Press.

Tian, L., Hires, S. A., Mao, T., Huber, D., Chiappe, M. E., Chalasani, S. H., et al. (2009). Imaging neural activity in worms, flies and mice with improved GCaMP calcium indicators. *Nature Methods*, *6*, 875–881.

Valmianski, I., Shih, A. Y., Driscoll, J. D., Matthews, D. W., Freund, Y., & Kleinfeld, D. (2010). Automatic identification of fluorescently labeled brain cells for rapid functional imaging. *Journal of Neurophysiology*, *104*, 1803–1811.

Vogelstein, J. T., Watson, B. O., Packer, A. M., Yuste, R., Jedynak, B., & Paninski, L. (2009). Spike inference from calcium imaging using sequential Monte Carlo methods. *Biophysical Journal*, *97*, 636–655.

Wallace, D. J., Zum Alten Borgloh, S. M., Astori, S., Yang, Y., Bausen, M., Kugler, S., et al. (2008). Single-spike detection in vitro and in vivo with a genetic Ca(2+) sensor. *Nature Methods*, *5*, 797–804.

Wang, Q., Shui, B., Kotlikoff, M. I., & Sondermann, H. (2008). Structural basis for calcium sensing by GCaMP2. *Structure*, *16*, 1817–1827.

Yaksi, E., & Friedrich, R. W. (2006). Reconstruction of firing rate changes across neuronal populations by temporally deconvolved Ca2+ imaging. *Nature Methods*, *3*, 377–383.

Yang, G., Pan, F., Parkhurst, C. N., Grutzendler, J., & Gan, W. B. (2010). Thinned-skull cranial window technique for long-term imaging of the cortex in live mice. *Nature Protocols*, *5*, 201–208.

Zhao, Y., Araki, S., Wu, J., Teramoto, T., Chang, Y-F., Nakano, M., et al. (2011). An expanded palette of genetically encoded Ca^{2+} indicators. *Science*, *333*, 1888–1891.